Hydrol. Earth Syst. Sci. Discuss., 10, 3283–3326, 2013
www.hydrol-earth-syst-sci-discuss.net/10/3283/2013/
doi:10.5194/hessd-10-3283-2013

Hydrology and Earth System Sciences
Open Access
Discussions

Potential surface temperature and shallow groundwater temperature response to climate change: an example from a small forested catchment in east-central New Brunswick (Canada)

B. L. Kurylyk[1], C. P.-A. Bourque[2], and K. T. B. MacQuarrie[1]

[1]Department of Civil Engineering and Canadian Rivers Institute, University of New Brunswick, Fredericton, New Brunswick, Canada
[2]Faculty of Forestry and Environmental Management, University of New Brunswick, Fredericton, New Brunswick, Canada

Received: 18 January 2013 – Accepted: 15 February 2013 – Published: 13 March 2013

Correspondence to: B. L. Kurylyk (barret.kurylyk@unb.ca)

Published by Copernicus Publications on behalf of the European Geosciences Union.

Abstract

Global climate models project significant changes to the air temperature and precipitation regimes in some regions of the Northern Hemisphere. These meteorological changes will have associated impacts to the surface and shallow subsurface thermal regimes, which are of interest to practitioners and researchers in many disciplines of the natural sciences. For example, groundwater temperature is critical for providing and sustaining suitable thermal habitat for cold-water salmonids. To investigate the surface and subsurface thermal effects of atmospheric climate change, seven downscaled climate scenarios (2046–2065) for a small forested catchment in New Brunswick, Canada were employed to drive the surface energy and moisture flux model, ForHyM2. Results from these seven simulations indicate that climate change-induced increases in air temperature and changes in snow cover could increase summer surface temperatures (range −0.30 to +3.49 °C, mean +1.49 °C), but decrease winter surface temperatures (range −1.12 to +0.08 °C, mean −0.53 °C) compared to the reference period simulation. Thus, changes to the timing and duration of snow cover will likely decouple changes in average annual air temperature (mean +2.11 °C) and average annual ground surface temperature (mean +1.06 °C).

The projected surface temperature data were then used to drive an empirical surface to groundwater temperature transfer function developed from measured surface temperature and depth-dependent groundwater temperature. Results from the empirical transfer function indicated that the change in groundwater temperature will exhibit seasonality at shallow depths (1.5 m), but be seasonally constant and approximately equivalent to the change in the mean annual surface temperature at deeper depths (8.75 m). The increases in future groundwater temperature suggest that the thermal sensitivity of baseflow-dominated stream to decadal climate change may be greater than previous studies have indicated. The ecological significance of these findings is discussed.

HESSD

10, 3283–3326, 2013

1 Introduction

1.1 Drivers and importance of ground surface temperature

The impact of climate change on ground surface temperature (GST) is of interest to a diversity of scientific disciplines. For example, hydrologists are concerned with the influence of surface freezing and thawing on infiltration and runoff rates (Williams and Smith 1989), agricultural scientists have shown that seed germination is affected by surface and near surface temperature (Mondoni et al., 2012), and geotechnical engineers have linked soil strength properties to surface/subsurface temperature (Andersland and Ladanyi, 1994). Increased GST could also enhance decay rates and CO_2 release from soils and thereby act as a positive feedback to climate change (Eliasson et al., 2005). Potential effects of changes in winter GST include: altered nutrient concentrations in soil water, enhanced winter root mortality, and decreased runoff quality (Mellander et al., 2007).

Increases in mean annual air temperature (MAAT) will not necessarily result in equivalent changes in mean annual GST (MAGST) (Mann and Schmidt, 2003; Mellander et al., 2007; Zhang et al., 2005); other physical processes must be considered to predict the associated increase in MAGST. For example, the duration of the snow-covered period is expected to decrease in northern latitudes due to increases in late fall and early spring air temperature (AT); this will reduce the insulating effect of the snowpack (Zhang, 2005) and alter the dynamics of atmosphere-surface heat exchange. A reduction in the snow-covered period would also lead to an increase in the amount of radiation absorbed by the ground (Bonan, 2008). The length of the growing season is also expected to increase with an upward shift in the AT regime in northern latitudes. Under a deciduous canopy, an increase in early-spring and late-fall foliation/defoliation could affect both thermal and hydrological processes by altering the amount of net radiation and evapotranspiration at the land surface (Bonan, 2008). The net effect of these positive and negative climate change feedback signals can be studied with a process-oriented model capable of simulating surficial thermal and hydrological processes.

HESSD
10, 3283–3326, 2013

Very few local-scale studies have investigated the impact of future climate change on GST regimes. Mellander et al. (2007) used two climate scenarios for 2091–2100, generated with the Hadley global climate model (GCM) and downscaled with a regional climate model (RCM), to predict changes in soil temperature in northern Sweden. They simulated a decrease in the period of persistent snowpack of 73–93 days, an increase in annual soil temperatures of 0.9–1.5 °C at 10-cm depth, and an advance in spring soil warming of 15–19 days. Salzmann et al. (2007) used the data from ten RCM-generated and two incremental climate scenarios to drive the surface energy balance model TEBAL and predicted a potential range of increased GST (mean +3.5 °C) for a mountainous permafrost region in Switzerland. Each of their RCM simulations were driven with the HadAm3H GCM forced by the A2 or B2 emission scenarios. They suggested that their study should be expanded by using multiple GCMs.

1.2 Drivers and importance of shallow groundwater temperature

The subsurface thermal regime is driven by water and energy fluxes across the ground surface and the geothermal flux from the earth's core. Seasonal and decadal variation in GST can be propagated downwards via conduction and advection and thereby perturb the temperature of shallow (i.e. < 10 m) groundwater (Taylor and Stefan, 2009). Thus, atmospheric climate change may result in changes to seasonal and mean annual GST (as discussed above), which could translate to shifts in the timing and magnitude of the seasonal groundwater temperature cycle.

Because groundwater temperature (GWT) is less variable than surface water temperature, groundwater discharge provides a thermal buffer for riverine systems during the summer and winter months (Caissie, 2006; Hayashi and Rosenberry, 2002; Webb et al., 2008). In eastern Canada, summer river temperatures are approaching the critical threshold for salmonids (Breau et al., 2007, 2011; Swansburg et al., 2004), and discrete cold-water plumes formed by groundwater-surface water interactions have been shown to provide critical thermal relief for cold-water fishes during high-temperature events (Breau et al., 2011; Cunjak et al., 2005; Ebersole et al., 2003; Torgersen et al.,

HESSD
10, 3283–3326, 2013

2012). As the climate warms, cold-water fishes may become increasingly dependent on groundwater-sourced thermal refugia.

Recently, there have been a number of publications investigating the thermal sensitivity of rivers to environmental conditions (e.g. Kelleher et al., 2012; Mayer, 2012; O'Driscoll and DeWalle, 2006; Tague et al., 2007). Many of these studies have demonstrated that groundwater-dominated streams are less sensitive to air temperature variability on a seasonal basis; however, the response of GWT (and consequently baseflow-dominated streams) to decadal climate change has not been well-studied. For example, Chu et al. (2008) stated "climate change induced differences in precipitation and temperature that may influence the magnitude and timing of groundwater discharge should be addressed in future analyses [of stream temperature]". Mayer (2012) acknowledged the dearth of information regarding the response of GWT to climate change and suggested that it posed a challenge for modelling future river temperatures.

Several researchers have attempted to address the impact of climate change on GWT. Taylor and Stefan (2009) employed an analytical solution to a simple conduction equation with a sinusoidal boundary condition to infer that the change in the mean annual GWT would be equivalent to the change in MAGST for Minnesota, USA. They suggested that the current seasonal amplitude of GWT would be relatively unchanged in a warmer climate. Gunawardhana et al. (2011) and Gunawardhana and Kazama (2011) employed an analytical solution to a one-dimensional conduction-advection equation with a linearly increasing GST to investigate the subsurface response to climate change in the Sendai Plain, Japan; however, this type of boundary condition does not allow for an investigation of seasonal trends in GWT. Gunawardhana and Kazama (2012) also used downscaled data from 15 GCMs to drive a numerical model (VS2DH) of groundwater flow and heat transport in the Sendai plain under multiple climate change scenarios. These simulations were performed on a coarse temporal resolution (1 yr) and did not address seasonal effects. Others (e.g. Bense et al., 2009; Ge et al., 2011) have simulated the impact of rising surface temperatures on permafrost degradation, but the

HESSD
10, 3283–3326, 2013

focus of these contributions has been the hydraulic evolution of shallow groundwater flow in suprapermafrost aquifers, rather than the thermal evolution.

1.3 Research objectives

The objective of this contribution is to provide answers to the following scientific questions:

1. Will changes in mean annual and seasonal GST closely mimic climate change-induced changes in mean annual and seasonal AT?
2. Can monthly GST data be utilised to predict monthly GWT in shallow aquifers by adopting an empirical approach?
3. How will shallow GWT respond to climate change on a monthly basis and what are the implications for salmonid thermal refugia?

These questions will be answered in reference to a small forested catchment with available field data (AT, GST, and GWT), and in which cold groundwater discharge has been observed to provide thermal refugia for salmonids. This work differs from previous GST studies by employing multiple GCMs and by investigating climate change impacts on surface processes in a warmer climate, albeit still with seasonal snow cover. The answer to the second equation will provide a simplistic alternative to implementing analytical solutions, which are replete with restrictions, particularly for the GST boundary condition. Finally, the answer to the third question should provide surface water hydrologists and ecologists with valuable information concerning the thermal sensitivity of baseflow-dominated rivers and the resilience of thermally-suitable fish habitat in a warming climate.

HESSD
10, 3283–3326, 2013

2 Study site

The geographic location selected for this study is the Catamaran Brook catchment (~ 53 km^2) in east-central NB, Canada (46° 52′ N latitude; 66° 06′ W longitude). Catamaran Brook is a third-order tributary of the Little Southwest Miramichi River (Fig. 1). The Catamaran Brook catchment has a mixed coniferous (65 %) and deciduous (35 %) Acadian forest cover (Cunjak et al., 1990). Portions of the catchment were clearcut in 1996 (Alexander, 2006). The annual average precipitation in the region is 1140 mm, with approximately 33 % falling as snow (Cunjak et al., 1993). The region experiences a humid continental climate with arid, cold winters and warm, humid summers (Cunjak et al., 1990).

As indicated in Fig. 2, the Catamaran Brook catchment is covered with a thin blanket of coarse sandy till, which is underlain by a dense clay till and Silurian and Devonian bedrock (Alexander, 2006). The water table is shallow and lies within the surficial sand and gravel deposit (Alexander, 2006).

Discharge in Catamaran Brook remains primarily groundwater-sourced throughout the year (Caissie et al., 1996). Because of the high degree of baseflow contributions, the water temperature of Catamaran Brook is generally considerably lower than that of the main stem of the Little Southwest Miramichi River, which has a high width to depth ratio and responds rapidly to solar radiation (Caissie et al., 2007). Juvenile Atlantic salmon (*salmo salar*) have been documented seeking thermal refuge in the cold-water plume at the mouth of Catamaran Brook during high temperature events (Breau et al., 2007). During a heat wave in 2010, very dense fish aggregations (> 10 000 fish) were observed in nearby thermal refugia within the Little Southwest Miramichi River (T. Linnansaari, UNB, personal communication, 2013).

HESSD
10, 3283–3326, 2013

3 Methods

3.1 Reference period and projected climate data

Future climate scenarios are generated by GCMs driven by emission scenarios that invoke assumptions about future population growth, technology, and economic development (Nakicenovic and Swart, 2000). GCM simulations are performed on coarse computational grids (e.g. 250 km by 250 km), thus their results should be downscaled to translate the data from the coarse grid to local climate conditions. Downscaling approaches have been thoroughly reviewed in the literature (e.g. Wilby and Wigley, 1997; Xu, 1999). A simple downscaling approach is the daily translation (DT) method, which is in the family of "statistical" or "quantile-quantile mapping" downscaling techniques (Teutschbein and Seibert, 2012). Statistical downscaling is predicated on the assumption that local climate conditions can be determined from large-scale climate variables using linear or non-linear transfer functions (Jeong et al., 2012a). In the DT method, a GCM is initially run for a reference period containing local observations. Scaling factors for precipitation and AT are then determined from the reference period simulations and local observations using empirical cumulative distribution functions. GCM simulations for a future time period (emission scenario) are then downscaled by applying the scaling factors.

Many more complex statistical downscaling methods have been developed; one of these is the hybrid multivariate linear regression (HMLR) method (Jeong et al., 2012a, b). In this method, the local climate variables are obtained from the GCM simulations using multiple regression functions determined from reference period simulations. Because regression-based methods often have difficulty producing the observed variability in local climate predictands, a stochastic generator is used to increase the variance in the datasets. These two methods (i.e. DT and HMLR) were employed in this study.

Output from GCMs can also be dynamically downscaled with RCMs; RCMs produce results on a finer computational grid than GCMs, using GCM output as boundary values. However, RCMs tend to introduce additional biases (Wilby et al., 2000). For

HESSD
10, 3283–3326, 2013

this reason, results from RCMs are often bias-corrected. This can be accomplished through techniques similar to those used for downscaling; in the present study, both of the dynamically-downscaled climate series (CRCM4.2.3 aev-A2 and CRCM 4.2.3 agx-A2, Table 1) were bias-corrected using the DT method addressed earlier.

The HMLR-downscaled data utilized in this study were contributed by the Université du Québec Institut National de la Recherche Scientifique (INRS, D. Jeong, personal communication, 2013), while the other climate data series were produced from the third Coupled Model Inter-comparison Project database of GCM output (CMIP3, Meehl et al., 2007) and dynamically downscaled using the Canadian Regional Climate Model (CRCM4.2.3, de Elia et al., 2008; Huard, 2011) or statistically downscaled with the DT method (Huard, 2011). In total, seven projected climate scenarios (Table 1) were produced for the period of 2046–2065 using six GCMs and one RCM, two downscaling methods, and three emission scenarios. These scenarios were selected because they span the range of plausible future climatic conditions for east-central New Brunswick. These climate data provide the basis for predicting future GST and GWT. The term "Run ID" (Table 1) refers to a particular simulation performed within the RCM; in this case, the primary difference between the two RCM runs (Agx and Aev) is the GCM driver (CGCM3 and Echam5).

Figure 3 provides the projected changes in mean annual precipitation and MAAT for each of the seven scenarios listed in Table 1. The observed climate data were taken from the Environment Canada (EC) database of adjusted and homogenized Canadian climate data (EC, 2010a). All of the scenarios predict a rise in MAAT (with range of 0.4–3.9 °C), but the projections for annual precipitation vary significantly in magnitude and direction (−15 to +50 %). It should be noted that the intent of this contribution is not to provide an in-depth analysis of the climate data but rather to drive the surface and subsurface models with multiple plausible climate scenarios produced with a variety of established methods. Thus, the intent is to examine the sensitivity of GST and GWT to external forcing rather than to make an assessment of the accuracy of predictions regarding the future state of surface and subsurface thermal regimes.

HESSD
10, 3283–3326, 2013

3.2 Physically-based model of surface temperature

The physically-based surface energy balance model ForHyM2 (Forest Hydrology Model v.2, Arp and Yin, 1992; Yin and Arp, 1993) was selected to simulate daily GST from meteorological data. ForHyM was originally developed for simulating water fluxes through shallow forest soils; this model successfully reproduced data from a deciduous forest in Ontario, Canada, and a coniferous forest in Quebec, Canada (Arp and Yin, 1992). Yin and Arp (1993) later developed ForSTeM, to simulate soil temperature. ForSTeM was created to be coupled to ForHyM, and these two models with subsequent revisions are collectively referred to as ForHyM2. ForHyM2 has been applied at many other sites (e.g. Balland et al., 2006; Bhatti et al., 2000; Houle et al., 2002; Meng et al., 1995; Oja et al., 1995) to simulate hydrologic fluxes and/or soil temperatures; model simulations closely agreed with field observations. ForHyM2 has also performed well at simulating snowpack depths under various forest canopies (Balland et al., 2006; Houle et al., 2002).

ForHyM2 requires daily AT, precipitation, and relatively few site characteristics for input conditions; thus simulations can be performed without extensive field work or site parameterization. Simulations can be started without initial conditions provided that the first timestep is not during a period with snow on the ground. ForHyM2 simulations were conducted in a simplified manner (one-dimensional) with the entire catchment represented as a point; thus surface heterogeneities were ignored. The observed climate data and the downscaled projected climate data were used to drive the ForHyM2 simulations on a daily time step. The GST was taken as the temperature of the forest floor surface. A more detailed description of the ForHyM2 model mechanics and input parameters is included in the Supplement.

3.3 Comparison of uncalibrated ForHyM2 simulations with measured GST

To test the accuracy of performing uncalibrated ForHyM2 GST predictions, simulated GST results were generated for a reference period and compared to observed GST.

HESSD
10, 3283–3326, 2013

Alexander (2006) installed temperature loggers (VEMCO Minilog) in the Catamaran Brook catchment to record hourly AT, GST, and GWT (see temperature loggers, Fig. 2). AT observations were recorded in shelters at a height of 1.5 m above the ground surface. GWT were recorded in the monitoring well indicated in Fig. 1; data loggers were installed at four depths: 1.5, 2.75, 5.25, and 8.75 m (Fig. 2). GST data were recorded near the monitoring well. The temperature data utilised in the present study were collected during 1 October 2001–30 September 2003. Additionally, measured precipitation data from the EC historical weather database for the Miramichi weather station (EC, 2010b) were used as input for the ForHyM2 simulations. In general, the ForHyM2-simulated GST time series agreed well with observed field data (Fig. 4). The associated coefficient of determination (R^2) was 0.98, thus ForHyM2 was judged to have performed favourably for these site conditions and meteorological data considering that no model calibration was undertaken.

3.4 Empirically-based estimation of groundwater temperature

Several previous studies investigating the impact of climate change on groundwater temperature have employed an analytical solution to the following governing equation for one-dimensional groundwater flow and heat transport (Domenico and Schwartz, 1990):

$$\lambda \frac{\partial^2 T}{\partial z^2} - q C_w \frac{\partial T}{\partial z} = C \frac{\partial T}{\partial t} \quad (1)$$

where λ is the thermal conductivity of the subsurface ($\mathrm{M\,L\,}t^{-3}\,T^{-1}$), T is the spatiotemporally varying groundwater temperature, q is the vertical Darcy flux ($\mathrm{L}\,t^{-1}$), C and C_w are the volumetric heat capacities of the medium and water, respectively ($\mathrm{M\,L}^{-1}\,t^{-2}\,T^{-1}$), z is depth (L), and t is time. Equation (1) has been analytically solved for GST that is linearly increasing on a decadal basis (Taniguchi et al., 1999) or periodically varying on a seasonal basis (Goto et al., 2005; Stallman, 1965). However, these

HESSD
10, 3283–3326, 2013

boundary conditions are inappropriate for the present study: linearly increasing GST ignores seasonal variations in temperature, and periodic (i.e. sinusoidal) GST is a poor approximation of the annual GST cycle in seasonally snow-covered catchments, due to the insulating effect of the winter snowpack (Lapham, 1989; Zhang, 2005). There are many other limitations associated with Eq. (1), including spatiotemporally constant groundwater flux and thermally homogeneous subsurface properties. Taylor and Stefan (2009) utilised a solution to a simplified form of Eq. (1) that ignored advective heat transport due to groundwater flow; however, advective heat transport could be significant in the Catamaran Brook basin, particularly in the shallow aquifer. The subsurface heat transport modelling capabilities in ForHyM2 (see supplementary material) were also not utilised for the present study because the model equations ignore advective heat transport due to groundwater flow.

In light of the limitations associated with the ForHyM2 model and the previously published analytical solutions, an empirical GST to GWT transfer function was adopted for simulating the monthly GWT response to rising GST:

$$\mathrm{GWT}_i = \mathrm{MAGST} + D\left\{\mathrm{GST}_{(i-L)} - \mathrm{MAGST}\right\} + B \quad (2)$$

where GWT_i is the GWT for month i, $\mathrm{GST}_{(i-L)}$ is the GST for month $(i-L)$, and D, L, and B are empirical parameters that are temporally constant, but depth-dependent. Although, this equation is empirically-based, the equation parameters relate to physical processes. Analytical solutions to the transient conduction equation have demonstrated that the seasonal GWT cycle is damped and lagged with respect to the seasonal GST cycle; the damping and lagging effects increase with depth (Bonan, 2008, p. 134; Taylor and Stefan, 2009). The unitless D parameter produces the damping effect of the subsurface thermal diffusivity, while the L parameter (units of months) produces the lagging effect between a GST-change and a GWT-realisation. The B term (°C) accounts for shallow heat transfer phenomena that may not be included in the other two parameters, which are conduction-based. These phenomena include: latent heat effects due

HESSD
10, 3283–3326, 2013

to freezing and thawing, vadose zone heat transfer processes in the vapour phase, and groundwater advection.

There are admittedly limitations to adopting an empirical approach for relating GST and GWT; however, linear and non-linear regression-based AT-stream temperature transfer functions have been developed for examining the response of surface water temperature to future warming climates (Kelleher et al., 2012; Mayer, 2012; Mohseni et al., 2003, and references therein). Furthermore, GST is the actual driver for shallow GWT temperature, whereas AT is merely used as a surrogate for radiation, the primary driver of river temperature (Allen and Castillo, 2007). Thus, the application of this GST-GWT transfer function should be as insightful as its surface water counterparts.

The measured GWT and GST temperature collected by Alexander (2006) were used to estimate the depth-dependent values of D, L, and B by minimizing the root-mean-square-error (RMSE) between the measured and simulated monthly GWT for each depth. It should be noted that two of the data loggers were installed in the sand and gravel aquifer, while the other two were installed in the clay aquitard (Fig. 2). Future projections of GWT at each depth were obtained by driving the GST-GWT transfer function with the future projections of GST obtained from ForHyM2. The flow of data from the GCMs to the GST-GWT transfer function is illustrated in Fig. 5.

4 Results

4.1 Projected climate change impacts on GST and snow cover

The most pronounced increase (2.64 °C) in MAGST, compared to the reference period simulated GST, was for the MIROC 3.2 HIRES-A1B climate data, while the only projected decrease in the MAGST (−0.15 °C) was obtained for the CSIRO Mk3.0-B1 climate data (Fig. 6). It should be noted that changes in MAAT for these particular scenarios were +3.96 and +0.39 °C, respectively (Fig. 3). Thus, it appears that the projected increases in MAAT are damped at the ground surface.

HESSD
10, 3283–3326, 2013

In addition to the projected variation in MAGST, the ForHyM2 results also suggest that changes will occur to seasonal GST. As indicated in Figs. 6 and 7, the trends in seasonal GST do not necessarily reflect the trends in MAGST. For example, the projected changes in MAGST are generally positive, whereas the trends in seasonal GST are typically positive for the spring, summer, and fall but negative for the winter. Additionally, Table 2 indicates that the changes in seasonal GST will not necessarily follow the changes in seasonal AT, although this appears to be the case in the summer.

Figure 8 indicates that the snow-cover period is expected to decrease under the various climate scenarios. The predicted reduction in the average snow-cover period could potentially range from 13 (CSIRO Mk3.0-B1) to 49 days (CRCM 4.2.3 AEV-A2). Additionally, Fig. 8 suggests that the mean annual average snowpack depth will also likely decrease. Estimated reductions in mean annual snowpack depth range from 35 % (CSIRO Mk3.0-B1) to 77 % (CRCM 4.2.3 AEV-A2). The simulated snowpack depths for the other five climate scenarios are within the range of the CSIRO Mk3.0-B1 and CRCM 4.2.3 AEV-A2 results.

4.2 GST-GWT transfer function

The best fit parameters for L, D, and B for each of the four depths are given in Table 3. Figure 9 gives plots for the measured and simulated monthly GWT at each of the four depths. The resultant correlation coefficient (R-value) and RMSE between the measured and simulated data are also indicated.

According to the analytical solution employed by Taylor and Stefan (2009), the lag term (L) and the natural logarithm of the damping term (D) should be linearly related to the depth. Figure 10 indicates that the L term and the natural logarithm of the D term obtained for the four depths can be reasonably approximated by a line with a zero intercept.

HESSD
10, 3283–3326, 2013

4.3 Projected climate change impacts on GWT

For the sake of clarity, only the GWT results from the reference period simulation (1961–2000) and the maximum (MIROC 3.2 HIRES-A1B) and minimum (CSIRO-Mk3.0-B1) simulated GWT are shown in Fig. 11. The GWT simulated from the MIROC 3.2 HIRES-A1B climate data exeeds the reference period GWT by approximately 1–3.5 °C depending on the month and depth, whereas the GWT simulated from the MIROC 3.2 HIRES-A1B climate is relatively unchanged from the reference period.

Figure 12 shows the change in average monthly GWT projected for each of the climate scenarios. As expected, the variability in the changes of monthly GWT decreases with depth for all climate scenarios.

5 Discussion

5.1 Relationship between climate-induced changes in AT and GST

Figures 3 and 6 demonstrate that the magnitude of the increases in projected MAAT for the seven climate scenarios (+0.4 °C to +3.9 °C) are larger than the simulated changes in MAGST (−0.15 °C to +2.64 °C). Thus, the findings of the present study concur with Mann and Schmidt (2003), who proposed the debated notion that decadal MAGST changes will not necessarily track MAAT changes (see Chapman et al., 2004; Schmidt and Mann, 2004). Decadal snow-cover evolution can decouple MAGST and MAAT trends by altering the average annual thermal resistance between the lower atmosphere and the ground surface. Figure 4 indicates that the variability in simulated and measured GST is considerably less in winter than in the other seasons due to the insulating effect of the snowpack; this effect is simulated in ForHyM2 by the inclusion of a thermal resistance layer during snow-covered periods (supplementary material). Figure 8 suggests that the snowpack insulating effect will likely be reduced in the coming decades due to a reduction in the snow-cover period and the average snowpack

HESSD
10, 3283–3326, 2013

depth. Thus, even when snow cover exists in a warmer climate, the equivalent thermal resistance will be limited by snowpack thinning. This will increase the winter heat transfer between the lower atmosphere and the ground surface and result in colder winter GST as indicated in Fig. 7a. This decrease in simulated winter GST limits increases in MAGST and may be an important negative climate change feedback for the subsurface thermal regime.

Table 2 indicates that changes in average summer GST (−0.30 to +3.49 °C) will closely replicate changes in average summer AT (−0.30 to +3.49 °C). Table 2 also suggests that increases in fall GST will be slightly less than increases in fall AT (average fall ratio, $\Delta GST/\Delta AT = 93\,\%$) and that increases in spring AT will be damped at the ground surface (average spring ratio, $\Delta GST/\Delta AT = 72\,\%$). The spring damping effect is presumably caused by a lingering snowpack. Thus, changes in seasonal GST will likely follow changes in seasonal AT during the warmer period, but not during the colder period.

5.2 The empirical GST-GWT function

The results presented in Fig. 9 indicate that an empirical relationship of the form of Eq. (2) is flexible enough to reproduce GWT at coarse spatial (∼ 2 m) and temporal (monthly) resolutions. As expected, the RMSE values were higher at shallow depths where the seasonal variability in GWT is greater; however, the relatively constant correlation coefficients (R-values) suggest that the function is consistent in addressing the variability in measured GWT to depths of approximately 9 m. Figure 9 suggests that the function has a problem with simulating GWT in April. We expect that this error arises due to advective heat transport associated with the spring snowmelt and major recharge event during this period and/or with the latent heat absorbed during the thawing of the upper few cm of soil.

The coefficients of determination (R^2) in Fig. 10 illustrate that the lag term (L) and the damping factor (D) generally varied with depth as expected. The slope of the natural logarithm of the damping factor vs. depth relationship can be used to infer a soil

HESSD
10, 3283–3326, 2013

thermal diffusivity of $7.1 \times 10^{-7}\,m^2\,s^{-1}$ (see Eq. 4 in Taylor and Stefan, 2009), which is in agreement with the typical saturated soil thermal diffusivity ($7.0 \times 10^{-7}\,m^2\,s^{-1}$) reported by Bonan (2008). Thus, the behaviour of the D and L terms concurred with our expectations based on classic heat conduction theory. As discussed, B is an encompassing parameter to account for any heat transfer process other than saturated zone conduction. Near-surface phenomena (freezing, evaporative losses to the atmosphere, thermal conductivity heterogeneities due to variable saturation, etc.) and groundwater flow can significantly perturb a temperature-depth profile. These phenomena exhibit seasonality, which would contribute to the errors in the estimated GWT for particular months. Table 3 indicates that the values of B decreased with increasing depth, which we expected given our proposition that B accounts for near-surface phenomena and advective heat transport. Clearly, the effects of near-surface phenomenon would decrease with depth; advective heat transport would also decrease with depth given the presence of the clay aquitard (Fig. 2). In general, the behaviour of the equation parameters (i.e. D, L, and B) is suggestive that they produce the physical effects that we postulated.

5.3 Shallow GWT respond to climate change

Figures 11 and 12 indicate that the MIROC 3.2 HIRES-A1B and CSIRO Mk3.0-B1 climate data resulted in the highest and lowest GWT, respectively. These results were consistent for each month and depth. This is not surprising given that these two climate scenarios also resulted in the highest and lowest MAAT (Fig. 3) and MAGST (Fig. 6). Thus, in general increased MAAT will result in increased MAGST and mean annual GWT; however, the response of monthly GWT to rising AT (and consequently rising GST) may be complex. For example, Fig. 12 indicates that at 1.5 m depth the maximum changes in the GWT for the MIROC 3.2 HIRES-A1B scenario (+3.43 °C) will occur in May, and the minimum changes in GWT (+1.26 °C) will occur in March. Thus, climate change-induced increases in shallow GWT will be seasonally dependent. Figure 12

HESSD
10, 3283–3326, 2013

demonstrates that this seasonality will decrease with depth; at 8.75 m, the increase in monthly GWT is approximately constant and equivalent to the rise in MAGST.

This study has also demonstrated that, due to increased summer GST and decreased winter GST (Fig. 7), the range in the annual cycle of GWT will increase. For example, the difference between the maximum (September) and minimum (February) average monthly GWT at a depth of 1.5 m was 13.8 °C for the reference period simulation; the differences projected for the seven climate scenarios ranged from 14.0 °C to 17.2 °C. These findings contrast with those of Taylor and Stefan (2009) who proposed that the amplitude of shallow GWT would not be significantly affected by a warming climate.

One motivation for this contribution was to examine the effect of rising GWT on groundwater-sourced salmonid thermal refugia. Stream temperature researchers have defined the thermal sensitivity of a stream as the slope of the AT-stream temperature relationship (e.g. Mayer, 2012). Following this approach, we define the subsurface thermal sensitivity (STS) as the ratio of the climate change-induced increase in summer GWT to the increase in summer AT. We are primarily concerned with summer temperatures, as this is the period when groundwater discharge is most critical for the preservation of salmonid populations (Breau et al., 2007; Cunjak et al., 2005). Table 4 presents the simulated STS for each climate scenario at each of the four depths. The STS values are negatively correlated with depth because simulated summer GST increases closely followed summer AT increases (Table 2), but simulated changes in MAGST were significantly damped compared to changes in MAAT. With increased depth, the subsurface thermal effect of seasonal GST is reduced, and the MAGST becomes the primary driver of GWT. The mean summer STS values for Catamaran Brook (0.66–0.88, Table 4) are somewhat higher than stream temperature sensitivities obtained by previous researchers examining air temperature-surface water temperature relationships (Kelleher et al., 2012; Mayer, 2012; O'Driscoll and DeWalle, 2006). For example, Kelleher et al. (2012) found that the average thermal sensitivity of smaller streams (0.52) was less than that of larger (stream order > 3) streams (0.83) for stream

HESSD
10, 3283–3326, 2013

systems in Pennsylvania, USA. Mayer (2012) used weekly AT and stream temperature data and found that the summer thermal sensitivities varied from 0.25 to 0.58 for six streams in Oregon, USA.

Kelleher et al. (2012, and references therein) proposed that thermal sensitivities of stream water temperature to AT variations derived from high frequency temperature data (e.g. seasonal, monthly, weekly, or daily) could be employed to estimate stream temperature sensitivity to climate change. This approach may not be valid in groundwater-dominated streams, because it is fundamentally based on the premise that GWT will respond in the same manner to both high frequency and low frequency AT variations. GWT may be insensitive to daily or even seasonal AT variations, but it is sensitive to decadal AT variations, as we have demonstrated by the aquifer STS values in Table 4. Thus many of the extrapolated seasonally-derived thermal sensitivities obtained for baseflow-dominated streams may underestimate the true thermal sensitivity to decadal climate change.

The changes in shallow (1.5 m or 2.75 m) summer GWT projected for the MIROC 3.2 HIRES-A1B data are approximately 3 °C (Fig. 12). Changes to the temperature of groundwater discharge on this order would increase local surface water temperature in groundwater-dominated streams and rivers by increasing the heat flux at the river bed (see Caissie et al., 2007; Hebert et al., 2011) and thereby affect local riverine ecosystems. Although GWT will respond to decadal climate change, groundwater-dominated tributaries will generally continue to remain colder than the main stems and thereby induce riverine thermal heterogeneity. Catchments for tributaries that provide thermal refugia should be protected from deforestation (Alexander, 2006; Bourque and Pomeroy, 2001) and aggregate extraction (Markle and Schincariol, 2007).

5.4 Limitations of the approach

Our modelling approach for estimating future GWT from GST assumes that the empirical parameters (B, D, and L) will be unaffected by a warming climate. It seems reasonable to assume that this will be the case for D and L based on the physical processes

HESSD
10, 3283–3326, 2013

they represent. The subsurface damping and lagging effects are primarily controlled by the period of the seasonal GST cycle, the soil diffusivity, and depth (Bonan, 2008); none of those controls will likely be significantly affected by atmospheric or surficial climate change. It is more likely that the *B* parameter would be affected by a warming climate. For example, increased precipitation and recharge rates could potentially lead to increased advective heat transport due to groundwater flow. At the latitude considered for this study, latent heat effects arising from pore-water phase changes may actually increase in a warmer climate, as winter GST are projected to decrease. As previously discussed, the importance of *B* decreases with depth, thus our simulations at deeper depths (e.g. 8.75 m) may be more reliable. Also, this empirical function assumes that the subsurface is in quasi thermal equilibrium with the surface; however, it could take years for the rise in MAGST to be fully realised in deeper (> 10 m) aquifer systems. These complex subsurface climate change feedbacks could also be simulated with physically-based groundwater flow and heat transport models that can accommodate freezing and thawing effects. We anticipate that this research will motivate others to perform additional studies in other aquifer-river systems.

6 Conclusions

To investigate the relationships between climate change and GST, simulations were conducted using the physically-based surface flux balance model ForHyM2. In general, the ForHyM2 results indicate that the changes in summer GST will mimic changes in summer AT. However, the model results also indicate that, due to complex snow-cover evolution effects, winter GST will likely decrease (−1.12 to +0.08 °C). This will result in MAGST changes (−0.15 to +2.64 °C) that are significantly damped with respect to MAAT changes (+0.39 to +3.96 °C).

Measured GWT and GST were used to develop an empirical relationship between the surface and subsurface thermal regimes. This empirical function was then driven with ForHyM2-produced GST projections to estimate the impact of atmospheric climate

HESSD
10, 3283–3326, 2013

change on GWT. Results from these simulations indicated that shallow (1.5 m) GWT is very sensitive to increases in summer AT. High frequency GST signals, such as seasonal variations in GST, are damped at greater depths; however, low frequency GST signals, such as decadal climate change, are retained at these depths. Thus, even GWT at deeper depths will respond to increasing AT and GST.

This study has also demonstrated the limitations inherent in predicting future climate change impacts using a single projected climate series based on one emission scenario, simulated with one GCM, and downscaled using only one approach. Climate modelling involves many assumptions and, as such, an array of climate scenarios should be considered.

We have also demonstrated that baseflow-dominated streams may be more sensitive to climate change than existing seasonally-derived thermal sensitivities, based on weekly air and stream temperature data, may indicate. Salmonids are threatened by rising river temperatures in eastern North America, and the ability of groundwater to buffer rising river temperatures may be overestimated. Future physically-based groundwater flow and heat transport modelling will be conducted to further investigate the potential increase in the temperature of groundwater discharge and the subsequent impact to cold-water fish habitat.

Supplementary material related to this article is available online at: http://www.hydrol-earth-syst-sci-discuss.net/10/3283/2013/hessd-10-3283-2013-supplement.pdf.

Acknowledgement. The climate data and information produced by Dae Jeong from Université du Québec Institut National de la Recherche Scientifique and David Huard from Ouranos are gratefully acknowledged. Paul Arp, Chengfu Zhang, and Fan-Rui Meng of the University of New Brunswick Watershed Group provided considerable assistance with the ForHyM2 model. Tommi Linnansaari, formerly a postdoctoral fellow with the Canadian Rivers Institute, provided valuable field-based information on fish aggregations within the thermal refugia of the Little

HESSD
10, 3283–3326, 2013

Southwest Miramichi River. This research has been funded by the Canada Research Chairs Program and a Natural Sciences and Engineering Research Council of Canada (NSERC) Collaborative Research and Development Grant. B. L. Kurylyk was also funded by NSERC postgraduate scholarships (Julie Payette PGS and CGSD3).

References

Alexander, M. D.: The thermal regime of shallow groundwater in a clearcut and forested streamside buffer, Doctorate of Philosophy Dissertation, University of New Brunswick, Department of Civil Engineering, Fredericton, NB, 436 pp., 2006.

Allen, J. D. and Castillo, M. M.: Stream Ecology: Structure and Function of Running Waters, Springer, Dordrecht, The Netherlands, 2007.

Andersland, O. B. and Ladanyi, B.: An Introduction to Frozen Ground Engineering, Chapman and Hall, New York, 1994.

Arp, P. A. and Yin, X.: Predicting water fluxes through forests from monthly precipitation and mean monthly air temperature records, Can. J. For. Res., 22, 864–877, doi:10.1139/x92-116, 1992.

Balland, V., Bhatti, J., Errington, R., Castonguay, M., and Arp, P. A.: Modeling snowpack and soil temperature and moisture conditions in a jack pine, black spruce and aspen forest stand in central Saskatchewan (BOREAS SSA), Can. J. Soil Sci., 86, 203–217, 2006.

Bense, V. F., Ferguson, G., and Kooi, H.: Evolution of shallow groundwater flow systems in areas of degrading permafrost, Geophys. Res. Lett., 36, 1–6, doi:10.1029/2009GL039225, 2009.

Bhatti, J. S., Fleming, R. L., Foster, N. W., Meng, F. R., Bourque, C. P. A., and Arp, P. A.: Simulations of pre- and post-harvest soil temperature, soil moisture, and snowpack for jack pine: comparison with field observations, For. Ecol. Manage., 138, 413–426, doi:10.1016/S0378-1127(00)00427-8, 2000.

Bonan, G.: Ecological Climatology, Cambridge University Press, United Kingdom, 2008.

Bourque, C. P.-A. and Pomeroy, J. H.: Effects of forest harvesting on summer stream temperatures in New Brunswick, Canada: an inter-catchment, multiple-year comparison, Hydrol. Earth Syst. Sci., 5, 599–614, doi:10.5194/hess-5-599-2001, 2001.

HESSD
10, 3283–3326, 2013

Breau, C., Cunjak, R. A., and Bremset, G.: Age-specific aggregation of wild juvenile Atlantic salmon *Salmo salar* at cool water sources during high temperature events, J. Fish Biol., 71, 1179–1191, doi:10.1111/j.1095-8649.2007.01591.x, 2007.

Breau, C., Cunjak, R. A., and Peake, S. J.: Behaviour during elevated water temperatures: can physiology explain movement of juvenile Atlantic salmon to cool water?, J. Anim. Ecol., 80, 844–853, doi:10.1111/j.1365-2656.2011.01828.x, 2011.

Caissie, D.: The thermal regime of rivers: a review, Freshwat. Biol., 51, 1389–1406, doi:10.1111/j.1365-2427.2006.01597.x, 2006.

Caissie, D., Pollock, T. L., and Cunjak, R. A.: Variation in stream water chemistry and hydrograph separation in a small drainage basin, J. Hydrol., 178, 137–157, doi:10.1016/0022-1694(95)02806-4, 1996.

Caissie, D., Satish, M. G., and El-Jabi, N.: Predicting water temperatures using a deterministic model: application on Miramichi River catchments (New Brunswick, Canada), J. Hydrol., 336, 303–315, doi:10.1016/j.jhydrol.2007.01.008, 2007.

Chapman, D., Bartlett, M., and Harris, R.: Comment on "Ground vs. surface air temperature trends: Implications for borehole surface temperature reconstructions" by M. E. Mann and G. Schmidt RID A-4103-2011, Geophys. Res. Lett., 31, L07205, doi:10.1029/2003GL019054, 2004.

Chu, C., Jones, N. E., Mandrak, N. E., Piggott, A. R., and Minns, C. K.: The influence of air temperature, groundwater discharge, and climate change on the thermal diversity of stream fishes in southern Ontario watersheds, Can. J. Fish. Aq. Sci., 65, 297–308, doi:10.1139/F08-007, 2008.

Cunjak, R. A., Caissie, D., and El-Jabi, N.: The Catamaran Brook habitat research project: description and general design of study, Department of Fisheries and Oceans, Gulf Region Science Branch, Moncton, NB, 14 pp., 1990.

Cunjak, R. A., Caissie, D., El-Jabi, N., Hardie, P., Conlon, J. H., Pollock, T. L., Giberson, D. J., and Komadina-Douthwright, S.: The Catamaran Brook (New Brunswick) habitat research project: biological, physical, and chemical conditions (1990–1992), Department of Fisheries and Oceans, Gulf Region Science Branch, Moncton, NB, 81 pp., 1993.

Cunjak, R., Roussel, J. M., Gray, M., Dietrich, J., Cartwright, D., Munkittrick, K., and Jardine, T.: Using stable isotope analysis with telemetry or mark-recapture data to identify fish movement and foraging, Oecologia, 144, 636–646, 2005.

HESSD
10, 3283–3326, 2013

de Elia, R., Caya, D., Cote, H., Frigon, A., Biner, S., Giguere, M., Paquin, D., Harvey, R., and Plummer, D.: Evaluation of uncertainties in the CRCM-simulated North American climate, Clim. Dynam., 30, 113–132, doi:10.1007/s00382-007-0288-z, 2008.

Domenico, P. A. and Schwartz, F. W.: Physical and Chemical Hydrogeology, Wiley, New York, 1990.

Ebersole, J. L., Liss, W. J., and Frissell, C. A.: Cold water patches in warm streams: physiochemical characteristics and the influence of shading, J. Am. Water Resour. Assoc., 39, 355–368, doi:10.1111/j.1752-1688.2003.tb04390.x, 2003.

EC: Environment Canada Historical Weather Database, http://www.climate.weatheroffice.gc.ca/climateData/dailydata_e.html?Prov=XX&timeframe=2&StationID=10808&Day=1&Month=1&Year=2010&cmdB1=Go, last access: October, 2010.

EC: Environment Canada Adjusted and homogenized daily Canadian climate data, available at: http://www.ec.gc.ca/dccha-ahccd/default.asp?lang=En&n=B1F8423A-1, last access: 20 July, 2011.

Eliasson, P. E., McMurtrie, R. E., Pepper, D. A., Stromgren, M., Linder, S., and Agren, G. I.: The response of heterotrophic CO_2 flux to soil warming, Glob. Change Biol., 11, 167–181, doi:10.1111/j.1365-2486.2004.00878.x, 2005.

Ge, S., McKenzie, J., Voss, C., and Wu, Q.: Exchange of groundwater and surface-water mediated by permafrost response to seasonal and long term air temperature variation, Geophys. Res. Lett., 38, 1–6, doi:10.1029/2011GL047911, 2011.

Goto, S., Yamano, M., and Kinoshita, M.: Thermal response of sediment with vertical fluid flow to periodic temperature variation at the surface, J. Geophys. Res.-Solid Earth, 110, B01106, doi:10.1029/2004JB003419, 2005.

Gunawardhana, L. N. and Kazama, S.: Climate change impacts on groundwater temperature change in the Sendai plain, Japan, Hydrol. Process., 25, 2665–2678, doi:10.1002/hyp.8008, 2011.

Gunawardhana, L. N. and Kazama, S.: Statistical and numerical analyses of the influence of climate variability on aquifer water levels and groundwater temperatures: the impacts of climate change on aquifer thermal regimes, Global Planet. Change, 86–87, 66–78, doi:10.1016/j.gloplacha.2012.02.006, 2012.

Gunawardhana, L. N., Kazama, S., and Kawagoe, S.: Impact of urbanization and climate change on aquifer thermal regimes, Water Resour. Manage., 25, 3247–3276, doi:10.1007/s11269-011-9854-6, 2011.

HESSD
10, 3283–3326, 2013

Hayashi, M. and Rosenberry, D. O.: Effects of ground water exchange on the hydrology and ecology of surface water, Ground Water, 40, 309–316, 2002.

Hebert, C., Caissie, D., Satish, M. G., and El-Jabi, N.: Study of stream temperature dynamics and corresponding heat fluxes within Miramichi River catchments (New Brunswick, Canada), Hydrol. Process., 25, 2439–2455, doi:10.1002/hyp.8021, 2011.

Houle, D., Duchesne, L., Ouimet, R., Paquin, R., Meng, F., and Arp, P. A.: Evaluation of the FORHYM2 model for prediction of hydrologic fluxes and soil temperature at the Lake Clair Watershed (Duchesnay, Quebec), For. Ecol. Manage., 159, 249–260, doi:10.1016/S0378-1127(01)00438-8, 2002.

Huard, D.: Climate change scenarios: thermal refuge for salmonids, Ouranos Report, Ouranos Consortium on Regional Climatology and Adaption to Climate Change, Quebec, Canada, 2011.

Jeong, D. I., St-Hilaire, A., Ouarda, T. B. M. J., and Gachon, P.: Multisite statistical downscaling model for daily precipitation combined by multivariate multiple linear regression and stochastic weather generator, Clim. Change, 114, 567–591, doi:10.1007/s10584-012-0451-3, 2012a.

Jeong, D. I., St-Hilaire, A., Ouarda, T. B. M. J., and Gachon, P.: A multivariate multi-site statistical downscaling model for daily maximum and minimum temperatures, Clim. Res., 54, 129–148, doi:10.3354/cr01106, 2012b.

Kelleher, C., Wagener, T., Gooseff, M., McGlynn, B., McGuire, K., and Marshall, L.: Investigating controls on the thermal sensitivity of Pennsylvania streams, Hydrol. Process., 26, 771–785, doi:10.1002/hyp.8186, 2012.

Lapham, W. W.: Use of temperature profiles beneath streams to determine rates of groundwater flow and vertical hydraulic conductivity, USGS Water Supply Paper# 2337, Denver, CO, 44 pp., 1989.

Mann, M. and Schmidt, G.: Ground vs. surface air temperature trends: implications for borehole surface temperature reconstructions, Geophys. Res. Lett., 30, 1607, doi:10.1029/2003GL017170, 2003.

Markle, J. M. and Schincariol, R. A.: Thermal plume transport from sand and gravel pits – potential thermal impacts on cool water streams, J. Hydrol., 338, 174–195, doi:10.1016/j.jhydrol.2007.02.031, 2007.

Mayer, T. D.: Controls of summer stream temperature in the Pacific Northwest, J. Hydrol., 475, 323–335, doi:10.1016/j.jhydrol.2012.10.012, 2012.

HESSD

10, 3283–3326, 2013

Meehl, G. A., Covey, C., Delworth, T., Latif, M., McAvaney, B., Mitchell, J. F. B., Stouffer, R. J., and Taylor, K. E.: The WCRP CMIP3 multimodel dataset – a new era in climate change research, B. Am. Meteorol. Soc., 88, 1383–1394, doi:10.1175/BAMS-88-9-1383, 2007.

Mellander, P., Lofvenius, M. O., and Laudon, H.: Climate change impact on snow and soil temperature in boreal Scots pine stands, Clim. Change, 89, 179–193, 2007.

Meng, F., Bourque, C. P., Jewett, K., Daugharty, D., and Arp, P. A.: The Nashwaak Experimental Watershed Project: analysing effects of clearcutting on soil temperature, soil moisture, snowpack, snowmelt and stream flow, Water Air Soil Pollut., 82, 363–374, doi:10.1007/BF01182847, 1995.

Mohseni, O., Stefan, H. G., and Eaton, J. G.: Global warming and potential changes in fish habitat in US streams, Clim. Change, 59, 389–409, doi:10.1023/A:1024847723344, 2003.

Mondoni, A., Rossi, G., Orsenigo, S., and Probert, R. J.: Climate warming could shift the timing of seed germination in alpine plants, Ann. Bot., 110, 155–164, doi:10.1093/aob/mcs097, 2012.

Nakicenovic, N. and Swart, R. (Eds.): Special report on emissions scenarios. A special report of Working Group III of the Intergovernmental Panel on Climate Change, Cambridge University Press, Cambridge, 2000.

NBADW: New Brunswick Aquatic Data Warehouse, available at: http://www.unb.ca/research/institutes/cri/nbaquatic/index.html, last access: October, 2012.

O'Driscoll, M. A. and DeWalle, D. R.: Stream-air temperature relations to classify stream-ground water interactions, J. Hydrol., 329, 140–153, doi:10.1016/j.jhydrol.2006.02.010, 2006.

Oja, T., Yin, X., and Arp, P. A.: The forest modelling series ForM-S: applications to the Solling spruce site, Ecol. Model., 83, 207–217, doi:10.1016/0304-3800(95)00099-H, 1995.

Salzmann, N., Noetzli, J., Hauck, C., Gruber, S., Hoelzle, M., and Haeberli, W.: Ground surface temperature scenarios in complex high-mountain topography based on regional climate model results, J. Geophys. Res.-Earth Surf., 112, 1–10, doi:10.1029/2006JF000527, 2007.

Schmidt, G. and Mann, M.: Reply to comment on "Ground vs. surface air temperature trends: Implications for borehole surface temperature reconstructions" by D. Chapman et al., Geophys. Res. Lett., 31, L07206, doi:10.1029/2003GL019144, 2004.

Stallman, R. W.: Steady one-dimensional fluid flow in a semi-infinite porous medium with sinusoidal surface temperature, J. Geophys. Res., 70, 2821–2827, doi:10.1029/JZ070i012p02821, 1965.

HESSD
10, 3283–3326, 2013

Swansburg, E., El-Jabi, N., Caissie, D., and Chaput, G.: Hydrometeorological trends in the Miramichi River, Canada: implications for Atlantic salmon growth, N. Am. J. Fish. Manage., 24, 561–576, doi:10.1577/M02-181.1, 2004.
Tague, C., Farrell, M., Grant, G., Lewis, S., and Rey, S.: Hydrogeologic controls on summer stream temperatures in the McKenzie River basin, Oregon, Hydrol. Process., 21, 3288–3300, doi:10.1002/hyp.6538, 2007.
Taniguchi, M., Shimada, J., Tanaka, T., Kayane, I., Sakura, Y., Shimano, Y., Dapaah-Siakwan, S., and Kawashima, S.: Disturbances of temperature-depth profiles due to surface climate change and subsurface water flow: 1. an effect of linear increase in surface temperature caused by global warming and urbanization in the Tokyo Metropolitan Area, Japan, Water Resour. Res., 35, 1507–1517, doi:10.1029/1999WR900009, 1999.
Taylor, C. A. and Stefan, H. G.: Shallow groundwater temperature response to climate change and urbanization, J. Hydrol., 375, 601–612, doi:10.1016/j.jhydrol.2009.07.009, 2009.
Teutschbein, C. and Seibert, J.: Bias correction of regional climate model simulations for hydrological climate-change impact studies: review and evaluation of different methods, J. Hydrol., 456–457, 12–29, doi:10.1016/j.jhydrol.2012.05.052, 2012.
Torgersen, C. E., Ebersole, J. L., and Keenan, D. M.: Primer for identifying cold-water refuges to protect and restore thermal diversity in riverine landscapes, US Environmental Protection Agency Report 910-C-12-001, Seattle, Washington, 78 pp., 2012.
Webb, B. W., Hannah, D. M., Moore, R. D., Brown, L. E., and Nobilis, F.: Recent advances in stream and river temperature research, Hydrol. Process., 22, 902–918, doi:10.1002/hyp.6994, 2008.
Wilby, R. and Wigley, T.: Downscaling general circulation model output: a review of methods and limitations, Prog. Phys. Geogr., 21, 530–548, doi:10.1177/030913339702100403, 1997.
Wilby, R., Hay, L., Gutowski, W., Arritt, R., Takle, E., Pan, Z., Leavesley, G., and Clark, M.: Hydrological responses to dynamically and statistically downscaled climate model output, Geophys. Res. Lett., 27, 1199–1202, doi:10.1029/1999GL006078, 2000.
Williams, P. J. and Smith, M. W.: The Frozen Earth: Fundamentals of Geocryology, Cambridge University Press, Cambridge, New York, 1989.
Xu, C.: From GCMs to river flow: a review of downscaling methods and hydrologic modelling approaches, Progress Phys. Geogr., 23, 229–249, doi:10.1177/030913339902300204, 1999.
Yin, X. and Arp, P. A.: Predicting forest soil temperature from monthly air temperature and precipitation records, Can. J. For. Res., 23, 2521–2536, doi:10.1139/x93-313, 1993.

HESSD
10, 3283–3326, 2013

Zhang, T.: Influence of the seasonal snow cover on the ground thermal regime: an overview, Rev. Geophys., 43, 1–23, doi:10.1029/2004RG000157, 2005.
Zhang, Y., Chen, W., Smith, S., Riseborough, D., and Cihlar, J.: Soil temperature in Canada during the twentieth century: complex responses to atmospheric climate change, J. Geophys. Res.-Atmos., 110, 1–15, doi:10.1029/2004JD004910, 2005.

HESSD
10, 3283–3326, 2013

Table 1. Details for each of the seven climate scenarios employed in the current study.

GCM (RCM)	GCM (RCM) Resolution	Run ID	Emission Scenario	Downscaling Approach	Contributor/ Reference
CGCM3	3.75 × 3.71°	–	A2	Statistical-HMLR	INRS (Jeong et al., 2012a)
CGCM3 (CRCM4.2.3)	3.75 × 3.71° (45 × 45 km)	Aev	A2	Dynamical	Ouranos (Huard, 2011)
ECHAM5 (CRCM4.2.3)	1.88 × 1.87° (45 × 45 km)	Agx	A2	Dynamical	Ouranos (Huard, 2011)
CSIRO Mk3.0	1.9 × 1.9°	–	B1	Statistical-DT	Ouranos (Huard, 2011)
CSIRO Mk3.5	1.9 × 1.9°	–	B1	Statistical-DT	Ouranos (Huard, 2011)
MIROC 3.2 HIRES	1.1 × 1.1°	–	A1B	Statistical-DT	Ouranos (Huard, 2011)
CGCM3	3.75 × 3.71°	–	A1B	Statistical-HMLR	INRS (Jeong et al., 2012a)

HESSD
10, 3283–3326, 2013

Table 2. Changes in seasonal[a] AT and ForHyM2-simulated GST for each climate scenario.

Climate Scenario	Winter (°C)		Spring (°C)		Summer (°C)		Fall (°C)	
	ΔAT	ΔGST	ΔAT	ΔGST	ΔAT	ΔGST	ΔAT	ΔGST
CGCM3-A2	3.31	−0.33	2.07	1.21	1.48	1.47	2.14	2.03
CRCM 4.2.3 aev-A2	4.34	−0.63	2.40	1.65	1.91	1.91	2.17	2.00
CRCM 4.2.3 agx-A2	2.05	−0.77	1.19	0.86	1.54	1.53	1.99	1.86
CSIRO MK3.0-B1	1.37	−0.71	0.32	0.28	−0.3	−0.30	0.18	0.13
CSIRO MK3.5-B1	1.81	−1.12	1.73	1.19	0.79	0.80	1.27	1.13
MIROC 3.2-HIRES-A1B	4.58	0.08	4.16	3.54	3.49	3.49	3.61	3.43
CGCM3-A1B	3.80	−0.21	2.05	1.29	1.54	1.54	2.36	2.14

[a] Winter = Dec–Feb, Spring = Mar–May, Summer = Jun–Aug, and Fall = Sep–Nov.

HESSD
10, 3283–3326, 2013

Table 3. Depth-dependent parameter values for the GST-GWT transfer function.

Depth (m)	Lag *L* (months)	Damping Term *D*	Empirical B (C°)
1.5	1.29	0.467	1.575
2.75	1.81	0.308	1.237
5.25	3.30	0.127	0.571
8.75	5.70	0.045	0.274

HESSD
10, 3283–3326, 2013

Table 4. Simulated summer subsurface thermal sensitivities (STS) for each depth, averaged for the seven climate scenarios.

Depth (m)	Average ΔGWT_s [a]	Average STS[b]
1.5	1.31 °C	0.88
2.75	1.26 °C	0.81
5.25	1.07 °C	0.72
8.75	0.98 °C	0.66

[a] ΔGWT_s refers to the average change in summer GWT (°C).
[b] STS refers to the summer subsurface thermal sensitivity: $STS = \Delta GWT_s / \Delta AT_s^c$.
[c] ΔAT_s refers to the average change in summer AT: ΔAT_s (°C) = 1.49 °C

HESSD
10, 3283–3326, 2013

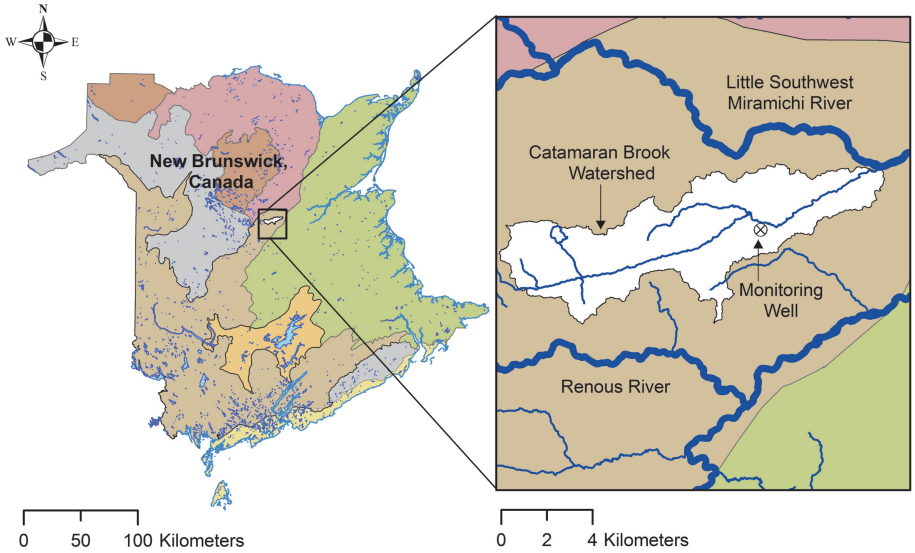

Fig. 1. Location of the Catamaran Brook watershed in New Brunswick, Canada; Catamaran Brook is located in the Valley Lowlands eco-region of New Brunswick (data from NBADW, 2011).

HESSD
10, 3283–3326, 2013

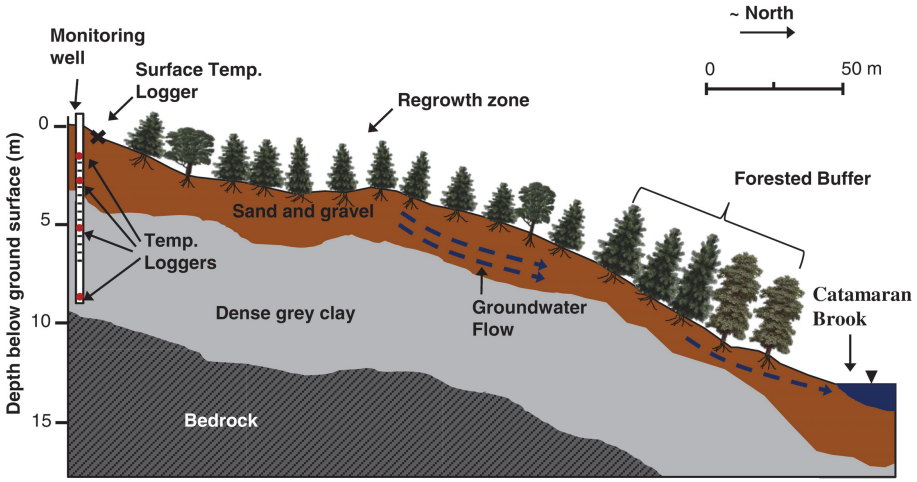

Fig. 2. Cross-sectional view of the portion of the Catamaran Brook catchment containing the monitoring well and temperature loggers (adapted from Alexander, 2006).

HESSD
10, 3283–3326, 2013

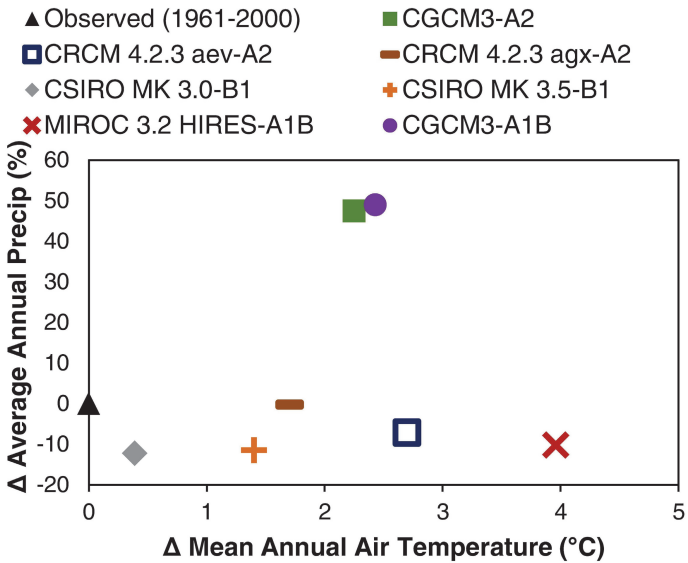

Fig. 3. Projected (2046–2065) changes in average annual precipitation vs. MAAT for east central New Brunswick in comparison to observations from 1961–2000.

HESSD
10, 3283–3326, 2013

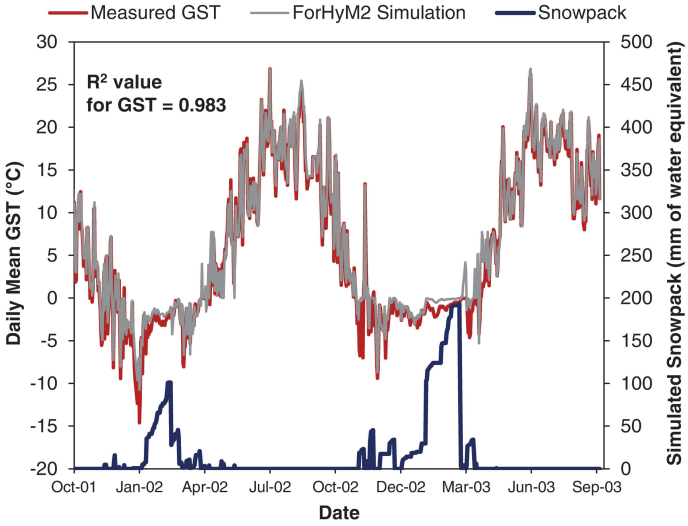

Fig. 4. Measured and ForHyM2-simulated GST and ForHyM2-simulated snowpack for the Catamaran Brook catchment over the October 2001-to-September 2003 period. GST data are relatively constant during the snow-covered period.

HESSD
10, 3283–3326, 2013

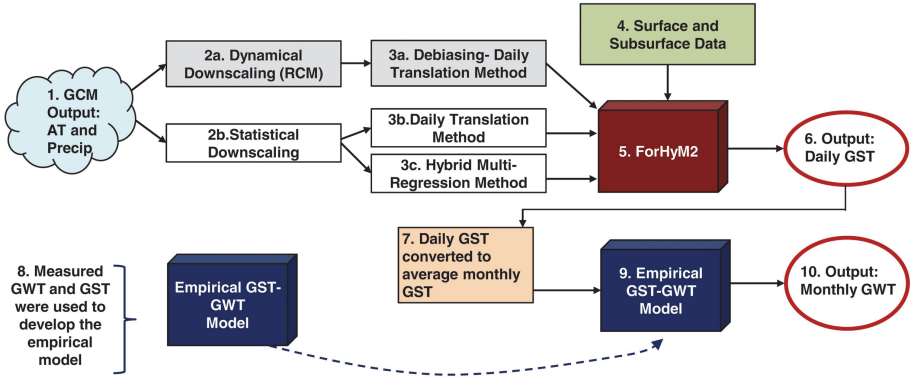

Fig. 5. Translation of GCM-simulated data into daily GST-simulations. Daily GST were summarized as monthly averages and entered as input to the empirical GST-GWT transfer function.

HESSD
10, 3283–3326, 2013

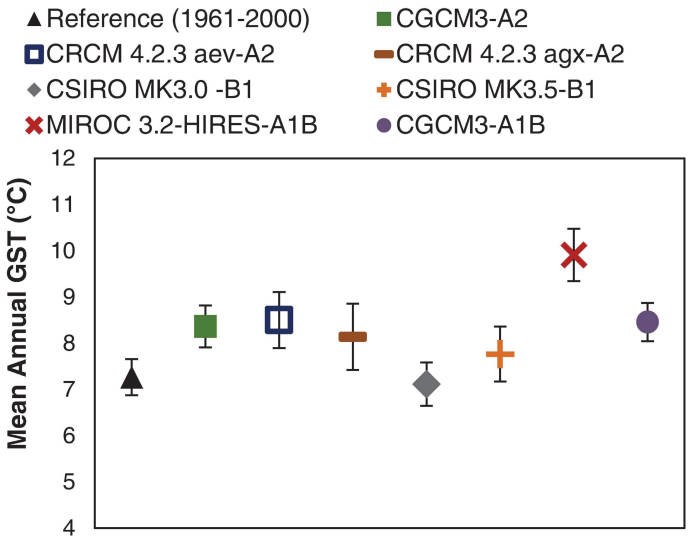

Fig. 6. ForHyM2-simulated MAGST for each climate scenario. Simulated MAGST based on historical climate data (1961–2000) is indicated by the data point to the far left; error bars indicate one standard deviation in MAGST.

HESSD
10, 3283–3326, 2013

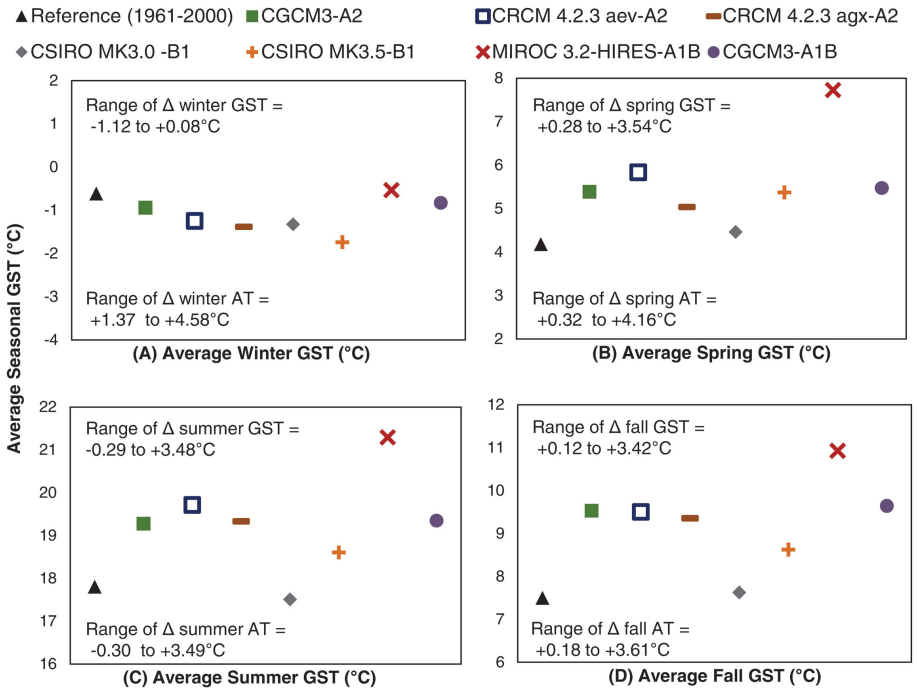

Fig. 7. ForHyM2-simulated average seasonal GST for each climate scenario and the reference period. The y-axes show various ranges in GST but are drawn to the same scale. Winter = December–February, Spring = March–May, Summer = June–August, and Fall = September–November.

HESSD
10, 3283–3326, 2013

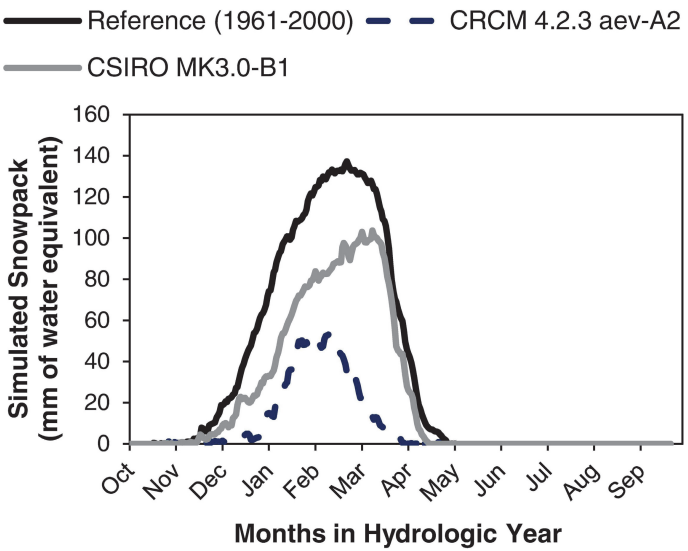

Fig. 8. ForHyM2-simulated snowpack depth (averaged over the duration of the simulation period) as a function of month, simulated snowpack depths for the other five climate scenarios are within the range set by the CSIRO Mk3.0-B1 and CRCM 4.2.3 AEV-A2 results.

HESSD
10, 3283–3326, 2013

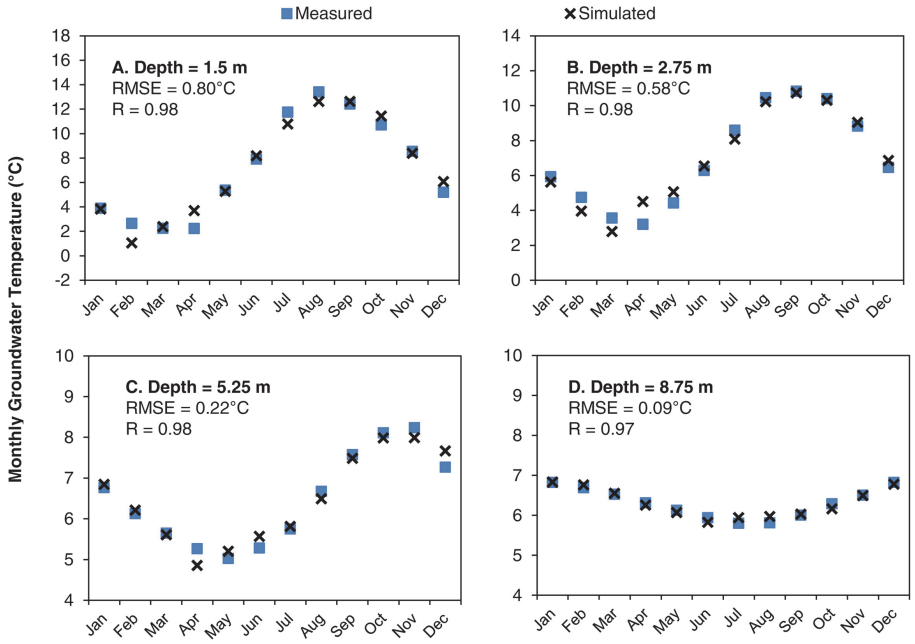

Fig. 9. Comparison of observed vs. simulated monthly GWT at different depths: **(A)** 1.5, **(B)** 2.75, **(C)** 5.25, and **(D)** 8.75 m. The y-axes are not all drawn to the same scale.

HESSD
10, 3283–3326, 2013

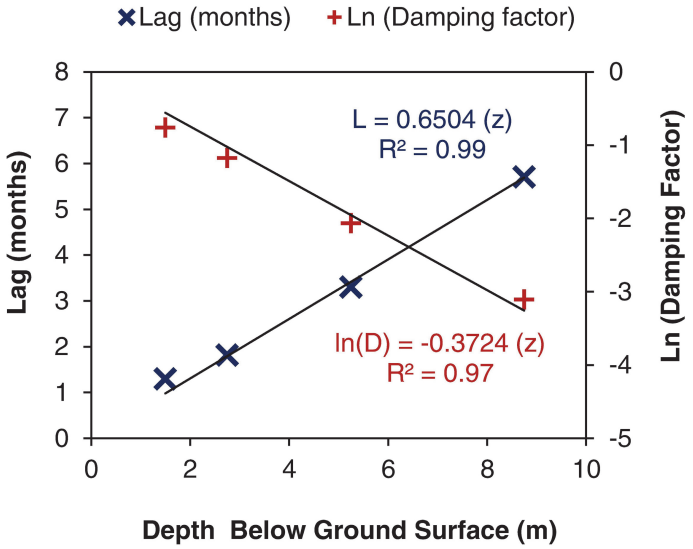

Fig. 10. The lag factor (L) and natural logarithm of the damping factor (D) plotted vs. depth (z). The L and D parameters were obtained from fitting Eq. (2) to measured GWT.

HESSD
10, 3283–3326, 2013

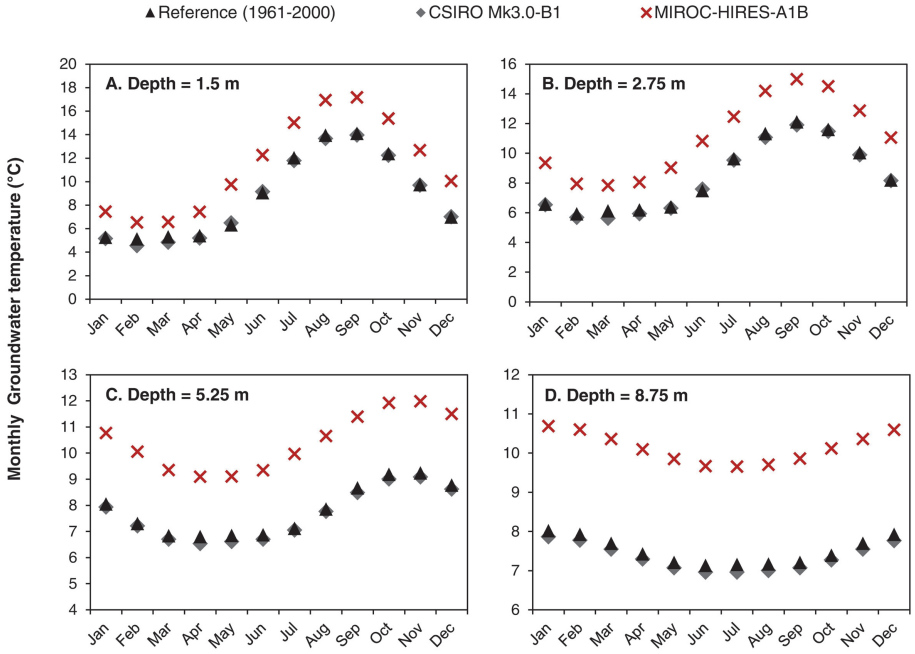

Fig. 11. Results from the empirical GST-GWT transfer function driven by the ForHyM2-produced GST temperature for the reference period and two projected climate scenarios. Of the seven climate scenarios, the CSIRO Mk3.0-B1 and the MIROC 3.2 HIRES-A1B climate scenarios consistently produced the lowest and highest monthly GWT, respectively.

HESSD
10, 3283–3326, 2013

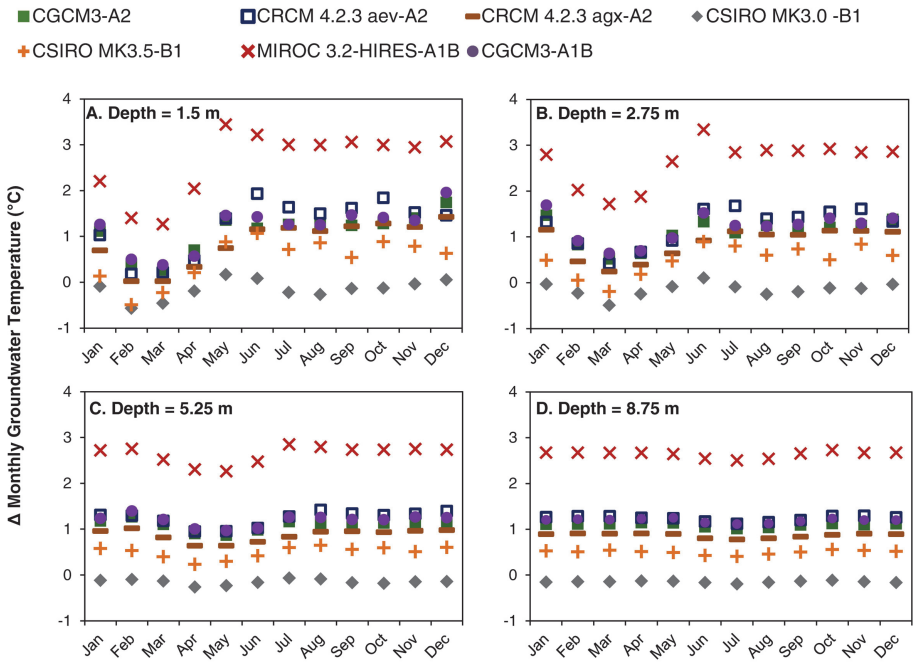

Fig. 12. Changes in monthly GWT produced by driving the GST-GWT transfer function with the projected GST data simulated for each of the seven climate scenarios.

HESSD
10, 3283–3326, 2013